

1 **ZEB1 shapes AML immunological niches suppressing CD8 T-cell activity while fostering Th17
2 cell expansion.**

3

4

5 **Running Title: ZEB1 promotes AML aggressiveness via immune suppression**

6

7 Barbara Bassani¹, Giorgia Simonetti², Valeria Cancila³, Marilena Ciciarello⁴, Annamaria Piva¹,
8 Claudia Chiodoni¹, Daniele Lecis¹, Alessandro Gulino³, Eugenio Fonzi⁵, Laura Botti¹, Paola
9 Portararo¹, Massimo Costanza⁶, Juerg Schwaller⁷, Alexandar Tzankov⁸, Maurilio Ponzoni⁹, Fabio
10 Ciceri⁹, Niccolò Bolli^{10,11}, Antonio Curti⁴, Claudio Tripodo³, Mario P. Colombo¹ and Sabina
11 Sangaletti¹.

12

13 **Affiliations**

14 1. Department of Research, Fondazione IRCCS Istituto Nazionale Tumori, Milan, Italy
15 2. IRCCS Istituto Romagnolo per lo Studio dei Tumori (IRST) "Dino Amadori" Meldola, Italy
16 3. University of Palermo School of Medicine, Palermo, Italy
17 4. Department of Experimental, Diagnostic and Specialty Medicine – DIMES, Institute of
18 Hematology " Seragnoli", Bologna, Italy
19 5. Unit of Biostatistics and Clinical Trials, IRCCS Istituto Romagnolo per lo Studio dei Tumori
20 (IRST) "Dino Amadori", Meldola (FC), Italy
21 6. Molecular Neuro-Oncology Unit, Department of Clinical Neuroscience, Fondazione IRCCS
22 Istituto Neurologico Carlo Besta, Milan, Italy
23 7. University of Basel Children's Hospital.
24 8. Institute of Medical Genetics and Pathology, University Hospital Basel, University of Basel, Basel,
25 Switzerland.
26 9. IRCCS Ospedale S. Raffaele; University Vita-Salute San Raffaele; Milan, Italy.
27 10. Hematology Division, Foundation IRCCS Ca' Granda Ospedale Maggiore Policlinico, 20122
28 Milan, Italy.
29 11. Department of Oncology and Hemato-Oncology, University of Milan, 20122 Milan, Italy

30

31 **Corresponding authors:**

32 Sabina Sangaletti
33 Fondazione IRCCS Istituto Nazionale dei Tumori
34 Via Giovanni Antonio Amadeo 42, 20133 Milan, Italy
35 Phone: +39 0223902212
36 Fax: +39 0223902630
37 sabina.sangaletti@istitutotumori.mi.it

38
39 Mario Paolo Colombo
40 Fondazione IRCCS Istituto Nazionale dei Tumori
41 Via Giovanni Antonio Amadeo 42, 20133 Milan, Italy
42 Phone: +39 0223902252
43 Fax: +39 0223902630
44 mariopaolet.colombo@istitutotumori.mi.it

45
46 **Keywords:** ZEB1, Acute myeloid Leukemia, IL-17, Microenvironment, Bone marrow

47

48 **Financial supports:** The research was supported by Associazione Italiana per la Ricerca sul Cancro
49 (ID.22204 project - PI Dr. Sangaletti Sabina and ID.22100 project – PI Dr. Chiodoni Claudia). BB is
50 funded by the FIRC-AIRC (Fondazione Italiana per la Ricerca sul Cancro) fellowship "Guglielmina

51 Lucatello e Gino Mazzega".

52

53 **Competing interests:** The authors declare that they have no competing interests.

54

55 **Word Count: 4319**

56 **Total number figures and tables: 7 Figures**

57

58 **ABSTRACT**

59 Acute myeloid leukemia (AML) development and progression is favored by immune suppression
60 directly triggered by leukemia cells. ZEB1 is a key transcription factor in epithelial-to-mesenchymal
61 transition which, we show here, is capable immune regulation in AML. Leukemic cells which had
62 ZEB1 knocked down have reduced engraftment and extramedullary disease when transplanted into
63 immune competent mice due to concomitant activation of CD8 T lymphocytes and reduced expansion
64 of Th17 cells. Differently, in ZEB1 competent AML, IL-17 sustains the development of a pro-
65 invasive and self-maintaining loop inducing *MMPs* and *SOCS2*. In humans, AML patients show, *in*
66 *situ* on bone marrow biopsies, a direct correlation between ZEB1 and Th17 and, in gene expression
67 profile when divided according to the median value of *ZEB1* expression, a different overall survival
68 and relapse along with the expression of MMPs, SOCS2 and Th17 cells enrichment. Overall, our data
69 shed new light into the role of ZEB1 in AML that entwines both pro-tumoral and immune regulatory
70 capacity in AML blasts.

71

72

73

74

75

76

77

78

79 **INTRODUCTION**

80 The bone marrow is a peculiar primary lymphoid organ in which the recirculation of naïve T-
81 cell and the presence of antigen-presenting cells competent for presentation may trigger anti-
82 leukemia T-cell responses. On this line, the number of T cells, present in the BM at diagnosis,
83 correlates with overall survival in newly diagnosed acute myeloid leukemia (AML)
84 patients(Lamble et al., 2020) (Davidson-Moncada et al., 2018) (Vadakekolathu et al., 2020).
85 Progression seen in AML suggests that immune suppressive mechanisms should be in place
86 overcoming anti-tumor T-cell response. In the hematopoietic niche, leukemic cells interact with
87 BM stromal cells establishing favorable conditions for survival, proliferation and resistance to
88 therapy as well as escape from immune recognition (Tettamanti et al., 2021) (Mendez-Ferrer et
89 al., 2020). As reported in solid tumors, potentially immunogenic leukemia cells seem to develop
90 multiple mechanisms for immune escape including the establishment of immune suppression.
91 These different immunomodulatory mechanisms encompass regulatory T cells, myeloid-
92 derived suppressor cells (MDSCs) (Han et al., 2014)engagement of inhibitory T-cells pathways
93 (i.e. PD-L1-/PD-1, arginase(Arg)-2 (Li et al., 2020) (Mussai et al., 2019)or interference with
94 specific metabolic pathways through indoleamine-2,3-dioxygenase (IDO (Curti et al., 2007).
95 The engagement of bystander cells, such as BM-MSCs, or a direct endogenous activity of AML
96 blast seem necessary to produce key factors capable of regulating immune cells activities.
97 ZEB1 has been extensively studied in solid cancers as a main transcription factor involved in
98 epithelial-to-mesenchymal transition (EMT) (Caramel et al., 2018).Recent evidences indicate
99 that ZEB1 could regulate also immune cell functions. Indeed, reciprocally to ZEB2, another
100 member of the ZEB family, ZEB1 is expressed by a variety of immune cells (Scott and
101 Omilusik, 2019)with immune suppressive functions. In tumor-associated macrophages
102 ZEB1seems to promote their polarization toward a pro-tumor phenotype (Cortes et al., 2017),
103 also its acts as repressor of miR-200, which negatively regulates the expression of the PD-L1
104 immune checkpoint (Chen et al., 2014). As mutated counterparts of normal myeloid cells
105 (Mussai *et al.*, 2019). AML blasts could adopt ZEB1 expression to modulate the leukemia
106 microenvironment. The expression of ZEB1 has been already reported in leukemia leading to
107 different and, sometimes, opposite conclusions, being ZEB1 described as both pro- and anti-
108 leukemogenic (Shousha et al., 2019) (Stavropoulou et al., 2016) (Li et al., 2021).
109 In this study, we functionally explored the impact of ZEB1 in murine leukemia cells seeding
110 the BM microenvironment and confirmed data and clinical relevance in AML patients.

111

112 **MATERIALS AND METHODS**

113

114 **Stable gene-silencing**

115

116 Lentiviral Particles were purchased from OriGene Technologies (catalog number TL513177V).
117 Two specific constructs (“seq-C” and “seq-D”) were tested for efficiency compared to a
118 negative control construct (“Scr”). For ZEB1 stable silencing in human K562 cells, we used the
119 Mission Lentivirus Transduction Particles (pLKO.1-shZEB1-565 - TRCN0000017565 and
120 pLKO.1-shZEB1-631 - TRCN0000364631), purchased from Sigma-Aldrich. A non-target
121 (Scramble - SHC003) sequence was used as negative control.

122

123 **Total RNA extraction, reverse transcription, and quantitative polymerase chain
124 reaction (qPCR)**

125 Total RNA was extracted using the Quick RNA micro prep kit (Zymo Research) and
126 subsequently quantified by NanoDrop 2000c Spectrophotometer (Thermo Scientific). cDNA
127 was generated using the high capacity Reverse Transcriptase kit (Applied Biosystems)
128 according to the manufacturer’s instructions. Taqman Probes used are listed in **Supplementary
129 Table 1**. Values were normalized to internal control (β -Actin) using the Δ CT method. For IL-
130 17A stimulation experiments, 5×10^4 human and murine cell lines expressing or silenced were
131 treated for 7 days with 50ng/mL rIL-17A. Untreated cells were used as control. $\Delta\Delta$ CT results
132 are shown. rIL-17A-stimulated cells were normalized to untreated cells.

133

134 **Gene expression profiling on murine cells**

135 Gene expression profiles were established by Thermo Fisher Mouse Clariom S Assay. RNA
136 labeling, processing, and hybridization were performed according to manufacturer’s
137 instructions, and microarrays were scanned with the Gene Chip System 3000 scanner. Raw data
138 were pre-processed using the sst-RMA algorithm implemented in the Transcriptome Analysis
139 Console software (Thermo Fisher). Downstream analyses were performed on pre-processed
140 data using R software. Multiple probes representing the same gene were collapsed by selecting
141 the probe with the highest variance across samples through the collapseRows function in the
142 WGCNA package (Miller et al., 2011). Differentially expressed genes (DEG) were identified
143 using limma package (Phipson et al., 2016). P-values were adjusted for multiple testing using
144 the Benjamini–Hochberg false discovery rate (FDR). Genes with an FDR <0.05 were
145 considered statistically significant. Gene set enrichment analysis (GSEA (Subramanian et al.,

146 2005)) was carried out in pre-ranked mode, according to the limma t-statistic, using the
147 hallmark gene set collection from the MSigDB database
148 (<http://software.broadinstitute.org/gsea/msigdb/index.jsp>). Gene sets with an FDR<0.05 were
149 considered statistically significant.

150

151 **Human gene expression datasets**

152 Public gene expression data were obtained from the Gene Expression Omnibus (GEO),
153 repository (<https://www.ncbi.nlm.nih.gov/gds>): GSE6891 (Verhaak et al., 2009), GSE12417,
154 GSE15434, GSE16015, GSE37642 (Li et al., 2013), GSE66525 (Hackl et al., 2015). NGS-
155 PTL (Next Generation Sequencing platform for targeted Personalized Therapy of Leukemia)
156 array data from 61 AML bone marrow samples (blasts $\geq 80\%$) have been previously generated
157 (Simonetti et al., 2021) (GSE161532) and patients characteristics are listed in **Supplementary**
158 **Table 2**. The Beat AML (Tyner et al., 2018) and The Cancer Genome Atlas project on AML
159 (Cancer Genome Atlas Research et al., 2013) transcriptomic cohorts were obtained from
160 <https://portal.gdc.cancer.gov/> (projects BEATAML1.0-COHORT and TCGA-LAML),
161 respectively. The datasets used in the manuscript are described in **Supplementary Table 3**.

162

163 ***In-vivo* AML murine models and bone marrow analysis**

164 Animal studies were approved by Institutional Committee for Animal Welfare and by the Italian
165 Ministry of Health and performed in accordance with national law D.lgs 26/2014 (authorization
166 n. 781/2018-PR). For the experiments involving C1498 intra-bone (i.b.) injection, at day 0,
167 2×10^5 Scr-C1498 or shZeb1-C1498 cells were injected into the tibia of immunocompetent mice.
168 After 34 days, mice were sacrificed.

169 For experiments using the IL-17A-neutralizing antibody, animals were injected with 5×10^5
170 Zeb1⁺ or silenced C1498. After 3 days, they were randomized. IL-17A–neutralizing or isotype
171 control Ab (50 μ g/mouse) were injected i.p. twice a week. Mice were sacrificed after 30 days
172 and BM and liver were explanted for further FACS analyses.

173 For the intracellular staining, the Foxp3/Transcription Factor Staining Buffer Kit (Tonbo
174 Biosciences) was used. Antibodies used for FACS analysis are listed in **Supplementary Table**
175 **1**. Samples were analyzed with the FACSCelesta flow cytometer equipped with FACSDiva
176 software (v 6.0) (Becton Dickinson). Flow cytometry data analyses were performed using
177 FlowJo software (v10.2).

178

179 **Statistical Analysis**

180 Statistical analyses have been performed with GraphPad Software (Prism 8). The statistic
181 applied to every single experiment is shown in the relative figure legend. Parametric and non-
182 parametric analysis (Student t test, Mann-Whitney test) have been applied according to data
183 distribution. A one-way ANOVA analysis with Tukey's or Dunnett's multiple comparison has
184 been applied according to multiple comparison.

185

186 **Data availability**

187 All data needed to evaluate the conclusions in the paper are present in the paper and/or the
188 Supplementary Materials. Microarray results are available in the National Center for
189 Biotechnology Information Gene Expression Omnibus repository (accession number
190 GSE192473).

191

192 **RESULTS**

193 **The median of *ZEB1* expression dichotomizes AML patients and defines patients with**
194 **worse OS and peculiar immune features.**

195 To define the relevance of *ZEB1* in AML we performed *in silico* analysis on 7 independent
196 cohorts from publicly available datasets (GSE15434, GSE16015, GSE12417, GSE37642,
197 GSE6891, GSE161532 and TCGA, **Supplementary Figure 1A**) for a total of 1325 AML
198 patients. AML patients were subdivided into two groups considering the median value of *ZEB1*
199 expression among patients to bisect *ZEB1*^{high} and *ZEB1*^{low} AML (**Figure 1A**). To identify the
200 main characteristics of *ZEB1*^{high} and *ZEB1*^{low} AML we performed a pathway analysis (**Figure**
201 **1B**) pointing out differences in the expression of immune response programs, including
202 inflammatory response, interferon gamma response, allograft rejection that were down-
203 regulated in *ZEB1*^{high} patients. On the contrary *ZEB1*^{high} patients showed an enrichment in
204 MYC, HEME metabolism, IL17A and TGF β pathways. Interestingly among genes
205 differentially expressed between *ZEB1*^{high} and *ZEB1*^{low} AML we found *MYC*, *SOCS2*,
206 *ARGINASE 2 (ARG2)* that were up-modulated in *ZEB1*^{high} patients (**Figure 1C**). Noteworthy,
207 *SOCS2* is relevant gene involved in controlling proliferation and stemness of HSC also marking
208 unfavorable leukemia (Vitali et al., 2015a) and *ARG2* was shown to be involved in the
209 polarization of monocytes into an immune suppressive M2-like phenotype in the leukemia
210 microenvironment (Mussai et al., 2013).

211 Of note, combining datasets for which the overall survival was available (GSE12417,
212 GSE37642, GSE6891, GSE161532 and TCGA) and for a total of 1298 patients, we found that
213 *ZEB1*^{high} AML patients had a shorter OS than *ZEB1*^{low} patients (**Figure 1D**). This finding was
214 also confirmed evaluating *ZEB1* through IHC in a small separated cohort of AML patients
215 (**Supplementary Figure 1B**).

216 Considering clinical features such as karyotype, French–American–British (FAB) classification
217 and overall survival (OS) of AML patients, we observed a significant difference between
218 *ZEB1*^{high} and *ZEB1*^{low} among cytogenetic subgroups (GSE6891, p=5.00E-07; TCGA-AML+
219 Beat AML, p=5.00E-07) (**Supplementary Figure 1C**), with a higher and lower percentage of
220 Normal Karyotype (NK)-and core-binding factor-mutated (CBF)-AML, respectively, in
221 *ZEB1*^{high} versus *ZEB1*^{low} cases. The different distribution according to FAB classification was
222 also confirmed (GSE6891, p=1.00E-07; GSE37642, p=4.60E-06; TCGA-AML+ Beat AML,
223 p=3.00E-07) (**Supplementary Figure 1C**), with *ZEB1*^{high} AML being enriched for more
224 undifferentiated leukemia types. The large number of cases in the cohorts of public datasets

225 allowed testing the association between *ZEB1* expression and the AML mutational profile.
226 *ZEB1*^{high} and *ZEB1*^{low} cases showed a similar frequency of *ASXL1*, *DNMT3A*, *IDH1*, *IDH2*,
227 *KRAS/NRAS*, *RUNX1*, *NPM1*, and *FLT3*-ITD mutations but differed for the concomitant
228 presence of *FLT3*-ITD and *NPM1* mutations: 15.8% vs. 5.8% in *ZEB1*^{high} vs. *ZEB1*^{low},
229 respectively (**Supplementary Figure 1D**). In line with cytogenetic data, *ZEB1*^{high} also included
230 a higher percentage of *TP53*-mut patients (13.5% vs. 3.6% of *ZEB1*^{low}, p=0.004), while *CEBPA*
231 biallelic mutations were only present in the *ZEB1*^{low} cohort (6.6% vs. 0% of *ZEB1*^{high}, p=0.003)
232 (**Supplementary Figure 1D**).

233 The data as a whole suggests that *ZEB1* might have an adverse impact on leukemia, potentially
234 due to alterations in the immune microenvironment that can encourage immunosuppression.
235

236 **Zeb1 silencing impairs the invasive ability of leukemic C1498 cells without affecting their
237 proliferation**

238 To model the activity of *ZEB1* in the context of leukemia, we started evaluating its expression
239 in two widely used, and well-characterized, AML murine cell lines, C1498 and WEHI-3B cells
240 (Mopin et al., 2016; Tomida, 1995). Western blot (WB) analysis (**Figure 2A**) and qPCR
241 (**Figure 2B**) showed high levels of *ZEB1*, both at protein and mRNA levels, in C1498 cells and
242 its paucity in WEHI-3B cells. Notably, the different expression of *ZEB1* in C1498 vs WEHI-
243 3B cells, correlated with the different expression of *Arg1* and *Tgfb*, which were higher in C1498
244 AML cells and lower in WEHI-3B, respectively (**Figure 2C**).

245 C1498 cells were stably silenced for *Zeb1* using a lentiviral vector also carrying a GFP tag to
246 allow FACS sorting of infected C1498-GFP positive cells. All target-specific shRNA
247 significantly decreased *Zeb1* expression compared to scramble transduced control (**Figure 2D**).

248 In a reverse approach, we tried to overexpress *Zeb1* in WEHI-3B cells. Despite efficient
249 transduction, according to GFP expression and *Zeb1* mRNA expression, (**Supplementary
250 Figure 2A**) WEHI-3B cells failed to express *ZEB1* protein (**Supplementary Figure 2B**).

251 Similar result has been obtained transducing *ZEB1* in human OCI-AML3 cells, in which
252 mRNA but not *ZEB1* protein was detectable upon gene transduction (not shown). Hence, we
253 focused on murine and human cell lines endogenously producing *ZEB1* and their silenced
254 counterpart because it was unfeasible to force *ZEB1* expression in low/negative cells.

255 Being *ZEB1* associated with tumor aggressiveness, proliferation, and differentiation properties,
256 we firstly investigated whether *Zeb1* silencing in C1498 cells could negatively impact cell
257 growth or invasiveness. *In vitro* experiments showed that *Zeb1* down-regulation did not affect

258 cell proliferation (**Figure 2E**) and only partially influenced C1498 differentiation state,
259 inducing a slight increase in CD11b, Ly6C and Ly6G expression (**Supplementary Figure 2C**).
260 Differently, *Zeb1* silencing significantly reduced the invasive properties of C1498 cells (**Figure**
261 **2F**), suggesting a possible role of ZEB1 in regulating the aggressiveness of AML cells.
262 Interestingly, a relevant effect of *Zeb1* silencing in C1498 cells was the decreased expression
263 of both *Tgfβ* and *Arg1* (**Figure 2 G-H**). Given the different behavior of *Zeb1*-expressing versus
264 silenced C1498 cells, we compared the gene expression profiles of our cell lines. Results
265 showed 56 up-regulated and 160 down-regulated genes in control versus sh*Zeb1*-seqC and 73
266 upregulated and 91 down-regulated genes in control versus sh*Zeb1*-seqD (**Figure 2I**). Notably,
267 *Zeb1* expressing cells had higher expression of genes related to *Myc* and *E2f* pathways or
268 involved in the mTOR signaling, compared with silenced counterpart (**Figure 2J**). Also, *Zeb1*-
269 expressing cells had a decreased expression of inflammatory and immune-related pathways,
270 among them *Tnf*, *Ifnα* and *Ifnγ* (**Figure 2J**). This data along with the down-modulation of *Arg1*
271 and *Tgfβ* in *Zeb1* silenced cells, suggests a possible involvement of ZEB1 in immune regulation
272 and particularly in immune suppression. To test the direct impact of ZEB1+ C1498 AML cells
273 on T cell activity, we performed a suppression assay in which αCD3 αCD28 stimulated CFSE-
274 labelled T cells were cultured with either *Zeb1*-silenced or *Zeb1*⁺ C1498 cells. Results show
275 that *Zeb1*⁺ cells more efficiently suppressed CD4⁺ and CD8⁺ T cell proliferation than sh*Zeb1*-
276 seqD-silenced cells (**Figure 2K**). Notably, the link between ZEB1 and immunosuppression via
277 Arginase I regulation was confirmed in myeloid derived suppressor cells (MDSCs), a subset of
278 myeloid cells that expand in solid tumors to mediate immune suppression (van Vlerken-Ysla et
279 al., 2023). Using a mammary tumor model previously characterized for the capacity to expand
280 MDSCs (Sangaletti et al., 2016) we show that *Zeb1* is highly expressed by MDSCs (**Figure 2L**).
281 ZEB1 protein level was higher in MDSCs isolated from the spleen of tumor-bearing mice than
282 in inflammatory neutrophils (Sangaletti et al., 2012) (**Figure 1M**). Notably, transient
283 knockdown of *Zeb1* in MDSCs (**Figure 2N**) was associated with decreased expression of *Arg1*
284 paralleled by increased *Il2* (**Figure 2N**), a T cell activating cytokine, at both transcriptional and
285 protein levels (ELISA, **Figure 2O**).
286

287 **Impaired BM engraftment of *Zeb1*-silenced AML cells is associated with cytotoxic CD8⁺
288 T cells expansion.**

289 To test the immune regulatory activity of ZEB1 *in vivo*, *Zeb1*-expressing (scramble transduced)
290 or -silenced (sh*Zeb1*) C1498 cells were injected orthotopically into the tibia of

291 immunocompetent, syngeneic C57BL/6 mice to better recapitulate the AML microenvironment
292 within the BM. Lower frequency of GFP⁺ leukemic cells was found in the BM of mice injected
293 with shZeb versus scramble transduced C1498 cells (**Figure 3A** for shZeb1-seqD and
294 **Supplementary Figure 3A** shZeb1-seqC). This finding was associated with reduced extent of
295 diffuse and nodular blast infiltration of liver parenchyma occurring in silenced versus control
296 injected groups, (**Figure 3B**). Notably, the silenced group, exemplified by shZeb1-seqD cells,
297 showed leukemic cells mostly confined around blood vessels, suggesting a limited invasiveness
298 of silenced than control cells (**Figure 3C**). A reduction in C1498 take was also observed in the
299 ovary of in mice injected with shZeb1-cells (**Supplemental Figure 3B**).
300 The relevance of Zeb1 in shaping the AML immune microenvironment was investigated by
301 multiparametric flow cytometry analysis performed on BM cells of mice injected *i.b.* with
302 shZeb1-silenced or Zeb1+ C1498 AML cells.
303 We found increased frequency of CD3+ cells in the BM of mice injected with Zeb1-silenced
304 than Zeb1+cells (**Supplementary Figure 3C**). This increase in T cells was not due to major
305 CD4+ cell increment (**Supplementary Figure 3D**), but mainly to a significant expansion of
306 CD8+ T cells in the BM of mice bearing shZeb1-seq-D cells versus scramble treated C1498
307 cells (**Supplementary Figure 2E-F**).
308 Looking at the CD8 subpopulations, we observed a higher frequency of CD8⁺PD1⁺ (**Figure**
309 **3D**) and CD8⁺IFN γ ⁺ (**Figure 3E**) T cells in the BM of mice receiving Zeb1-silenced than Zeb1+
310 control cells. Since PD1 is expressed on activated CD8 T-cells but it is also a marker of
311 exhaustion, another marker of exhaustion, such as TIM3, was evaluated along with the ability
312 to produce IFN γ . We found increased CD8⁺PD1⁺Ki67⁺IFN γ ⁺ cell fraction (**Figure 3F** and
313 **Supplementary Figure 3G**). Concomitantly, the reduction of PD1⁺TIM3⁺ cell frequency
314 (**Figure 3G and Supplementary Figure 3H**) in the BM of mice injected with Zeb1 silenced
315 cells confirms that Zeb1 down-regulation in leukemic cells unleashes the expansion of activated
316 T cells. Accordingly, the frequency of OX40+CD8+ lymphocytes was higher in BM injected
317 with Zeb1-silenced cells than controls (**Figure 3H**).
318 The activation of CD8⁺ T cell in the BM was supported by qPCR analysis performed on total
319 BM cells showing the up-regulation of *Perforin1* (*Prf1*) and *Ox40L* (*tnfsf4*) and a trend in
320 increase of *Granzyme B* and *Tnf* (**Figure 3I-L**) in mice injected with shZeb1-seq D compared
321 with controls. This phenotype was paralleled by the decrease of genes encoding for
322 immunosuppressive molecules, including *Arg1* and *Il10* (**Figure 3M-N**).
323

324 **IL17A is responsible for ZEB1-driven extramedullary infiltration of leukemia cell *in-vivo*.**
325 To further characterize ZEB1-dependent immunosuppressive effect on the BM
326 microenvironment, we also analyzed the CD4⁺ population in the BM of mice injected with
327 shZeb1-silenced or scramble transduced C1498 AML cells. Although the overall frequency of
328 CD4 T cells was non different, the fraction of Treg cells was slightly reduced (**Figure 4A**) in
329 favor of a statistically significant expansion of TNF-producing CD4⁺ cells (**Figure 4B**) and a
330 trend toward increase of IFN- γ ⁺ CD4⁺ (**Figure 4C**) cells in the *Zeb1*-silenced group.
331 Furthermore, an expansion of CD3⁺IL-17⁺, Th17, and Treg IL-17⁺ T cells occurred in the BM
332 of mice injected with ZEB1+ control cells in comparison to *Zeb1* silenced AML cells or normal
333 mice (**Figure 4D-F and Supplementary Figure 3I-J**).
334 This data might be explained by the significant down-modulation of *Il6* and *Il23A* in *Zeb1*-
335 silenced cells (**Figure 4G**), which together with *Tgf β* are the main regulator of Th17
336 differentiation (Geginat et al., 2016). To test the relevance of IL-17A production by CD3⁺,
337 CD4⁺, and Tregs on AML growth and dissemination *in-vivo*, IL-17A neutralizing or isotype-
338 matching mAbs were given every 3 days to mice implanted with *Zeb1* competent and silenced
339 cells (**Figure 4H**).
340 In mice injected iv, IL-17A blockade slightly reduced leukemic cell take in the BM (**Figure 4I**)
341 but significantly impaired the infiltration of C1498 cells to the liver compared to mice treated
342 with the isotype control only in Scramble injected mice (**Figure 4J**). The almost unchanged
343 engraftment of C1498-GFP cells in presence of a strong reduction in liver spreading under
344 treatment with anti-IL-17A-neutralizing Abs, suggests a major role of IL-17A in AML
345 dissemination.
346 To better understand how IL-17A promotes AML dissemination in relation to ZEB1
347 expression, *Zeb1*-silenced and *Zeb1*+ C1498 cells were stimulated with mrIL-17, and tested for
348 cell proliferation. Interestingly, rIL17 significantly increased the proliferation of *Zeb1*⁺ cells
349 (**Figure 5A**) and the expression of *Socs2*, which of note was one of the relevant gene
350 differentially expressed among *ZEB1*^{high} and *ZEB1*^{low} AML patients, and *mmp9* the latter is
351 relevant marker of AML (Pirillo et al., 2022) also directly associated to blast invasion (Feng et
352 al., 2011) (**Figure 5B**). In addition, rIL-17 exposure also induced *Il6* and *Tgf β* expression
353 (**Figure 5C**), thus supporting the idea that AML cells can self-activate a Th17-maintaining
354 loop. Notably, the expression of IL17A receptor remained unchanged in *Zeb1*-silenced and
355 *Zeb1*+ cells (**Supplementary Figure 4A**).
356

357 To corroborate our mouse data in the human setting, we initially investigated ZEB1 expression
358 in a panel of 6 different leukemic cell lines. Among them, only the K562 was expressing ZEB1
359 (**Figure 5D**) allowing the generation of its *ZEB1*-silenced counterpart (**Figure 5E**). Although
360 without differences in the surface markers (**Supplementary Figure 4B**), the *ZEB1*-silenced
361 variant showed reduced expression of *SOCS2*, *TGFβ* and of *IL23*, a cytokine involved in Th17
362 maintenance (**Figure 5F**) (Stritesky et al., 2008). As for murine AML cells, rhIL17 stimulates
363 K562 cell proliferation (**Supplementary Figure 4C**) in association with up-regulation of
364 *SOCS2*, *MMP9*, and *IL6*, but not *TGFβ* (**Figure 5G, H**).

365
366 To identify the direct targets of ZEB1 among molecules affected during its silencing, we
367 performed Chromatin immunoprecipitation (ChIP) experiment followed by a qPCR on the
368 obtained DNA. With this experiment, in human K562 cells, we were able to validate the
369 binding of ZEB1 to the promoter of *SOCS2* and *IL23A* (**Figure 5I**). Notably, we further
370 confirmed these data also analyzing publicly available Chip-seq data, which although
371 performed on lymphoma cells (GM12878), confirmed the direct binding of ZEB1 to the
372 promoter of *SOCS2* and *IL23A* (**Supplementary Figure 4D**).

373 To further challenge the association between ZEB1 expression in leukemic blasts and Th17,
374 we performed a double IF staining on archival BM biopsies from 26 AML patients divided into
375 ZEB1^{high} and ZEB1^{low} according to the median number of ZEB1+ nuclei, which ranged from
376 0.5 up to 60% (**Figure 6A**). Notably, we found a higher number of CD3⁺IL-17⁺ cells in
377 ZEB1^{high} than ZEB1^{low} AML cases (**Figure 6B, C**) with a positive correlation between ZEB1
378 levels and the number of CD3⁺IL-17A⁺ cells (**Figure 6D**). Accordingly, a gene signature able
379 to identify Th17 cells in TSGA AML cohorts using the GEPIA2 tool revealed an association
380 with poor outcome in terms of overall survival (**Figure 6E**) in patients enriched for this
381 signature.

382
383 **Relevance of Th17-ZEB1 axis in AML relapse**
384 Given the known activities of ZEB1 in drug resistance (Meidhof et al., 2015) we investigated
385 its possible role in AML relapse. We performed in silico studies using gene expression profiling
386 (GEP) analysis on paired AML blasts obtained at diagnosis and relapse (GSE66525) (Hackl *et*
387 *al.*, 2015). We found a further increase in ZEB1 expression in relapsed samples (**Figure 7A**),
388 along with a trend of increased MMP2 and SOCS2 expression (**Figure 7B-C**). Interestingly, in
389 the same patients, the higher ZEB1 levels in relapsed patients were associated with the
390 enrichment in the Th17 pathway (**Figure 7D**). Moreover, investigating the differentially

391 expressed hallmarks at relapse compared with diagnosis, we found an up-regulation of MYC
392 targets and UV response, and a downregulation of inflammatory response, allograft rejection,
393 and interferon gamma response (**Figure 7E**), all pathways related to ZEB1-positive blasts. This
394 finding supports the hypothesis that relapsed AML is enriched in ZEB1-positive blasts and
395 maintains the ZEB1-driven Th17 skewing.

396

397 **Discussion**

398 Nowadays it is widely accepted that AML cells can influence the BM microenvironment to
399 their own advantage such to create a peculiar niche that supports their survival, resistance to
400 therapy and immune evasion. Nevertheless, beside IFN γ , no other molecular drivers active in
401 molding the BM immune microenvironment under AML influence have been characterized in
402 depth (Corradi *et al.*, 2022; Vadakekolathu *et al.*, 2020). Here, we demonstrate a formerly
403 undiscovered ability of the EMT-regulator ZEB1 to shape the BM immune microenvironment,
404 when expressed by leukemic blasts, sustaining AML progression. Our data indicate that ZEB1
405 directly orchestrates T-cell suppression via Arginase, and promotes Th17 expansion; the
406 combination of these features negatively affects patients' OS.

407 Previous studies performed on AML characterized by the *MLL-AF9* fusion gene, showed ZEB1
408 expression associated with aggressive LT-HSC-derived AML, and with reduced OS. Regarding
409 the potential oncogenic activity of ZEB1 in AML (Li *et al.*, 2021) (Shousha *et al.*, 2019)
410 (Stavropoulou *et al.*, 2016) discordant evidences have been published. Almotiri and coll.
411 postulated that ZEB1 acts as a transcriptional regulator of haematopoiesis and that its
412 expression is required to suppress leukemic potential in AML models (Almotiri *et al.*, 2021).
413 This data might fit with our inability of over-expressing ZEB1 protein despite efficient gene
414 transduction and mRNA expression in both mouse and human cell lines that endogenously are
415 low/negative for Zeb1. Differently, the possibility of silencing ZEB1 where it is spontaneously
416 expressed suggest a cell-dependent protein dosage limitation. Our analysis of *ZEB1* expression
417 and distribution in larger datasets, including those evaluated by Almotiri and coll., showed that
418 not all AML patients express *ZEB1* at level lower than healthy controls. Rather, a fraction of
419 them expresses significantly higher levels of *ZEB1* than controls, particularly in the CN-AML
420 cohorts. Also, our IHC/IF analyses confirmed higher inter-patient variability with some patients
421 showing positivity for ZEB1 protein in almost all blasts and other patients showing ZEB1
422 expression confined to few blasts. To better dissect the biological and clinical features
423 associated to *ZEB1*^{high} AML, we analyzed *in silico* data and dichotomized patients in two
424 groups according to the median level of *ZEB1* expression that also bisects OS, FAB and
425 karyotypes. At molecular level, *ZEB1*^{high} AML patients showed increased expression of
426 pathways related to the Myc, SOCS2, IL-17, TGF β and HEME metabolism and down-
427 modulation of inflammatory pathways. The last combined to the up-regulation of ARG2 gene
428 in *ZEB1*^{high} AML have suggested the ZEB1 could entwines both pro-tumoral and immune
429 suppressive features in AML that were accordingly demonstrated in immune competent mice.

430

431 In the C1498 AML mouse model, knock-down of *Zeb1* revealed that ZEB1+ leukemia cells
432 may hinder the activity of CD4 and CD8 T-cells by directly modulating *Arg1* expression.
433 Although the direct binding of ZEB1 to the *Arg1* promoter was not demonstrated, the observed
434 decrease in *Arg1* expression resulting from transient silencing of MDSCs strongly supports this
435 hypothesis. Additionally, in humans, the co-regulation of ZEB1 with ARG2 and the ENCODE
436 project's identification of ARG2 as one of ZEB1's target genes further supports the notion that
437 ZEB1 functions as a regulator of Arginase. Arginase 2 is a protein involved in several cellular
438 functions, including polyamine synthesis and cellular energy metabolism. Although it is not
439 completely elucidated whether it directly suppress immune function, its interaction with other
440 molecules or cellular pathways can have indirect effects on immune function (Dowling *et al.*,
441 2021; Grzywa *et al.*, 2020). In acute myeloid leukemia (AML), an increased expression of
442 Arginase 2 in blasts contributes to chemotherapy resistance suppressing immune responses by
443 polarizing surrounding monocytes into a suppressive M2-like phenotype (Mussai *et al.*, 2013).
444 Therefore, whether Arginase 1 and 2 might play similar or divergent functions also according
445 to their cellular source and species remains unclear. Interestingly, arginase 1 has been involved
446 in the differentiation of Th17 (Wu *et al.*, 2016), which along with immune suppression
447 represented the main features associated to ZEB1^{high} AML. It is noteworthy that, in both human
448 and murine models, Th17 cells promoted the expression of SOCS2, a gene that is involved in
449 the aggressiveness of leukemia (Vitali *et al.*, 2015a; Vitali *et al.*, 2015b). In this case, our Chip-
450 qPCR analysis, along with data from the ENCODE project, demonstrated the direct binding of
451 ZEB1 to the promoter of SOCS2 and IL23.
452 In humans, Th17 are prognostically relevant in AML and other cancers (Civini *et al.*, 2013)
453 (Han *et al.*, 2014). Musuraca *and coll.* described a population of IL-17/IL-10-secreting immune
454 suppressive Th17-cells that could identify AML patients with a higher risk of severe infections
455 and relapse (Musuraca *et al.*, 2015). The increase in ZEB1, along with Th17, SOCS2, and
456 MMP2, in blasts at relapse compared to diagnosis, leads to the conclusion that ZEB1 expression
457 in AML may be particularly relevant in identifying patients who are at a higher risk of relapse
458 after chemotherapy and, more importantly, after allogeneic hematopoietic stem cell
459 transplantation (HSCT). Even the improvement in the treatment, relapse still represents a
460 common scenario in AML, occurring in 40–50% of younger and the great majority of elderly
461 patients (Thol and Ganser, 2020). This relapse usually arises within the bone marrow, even if
462 increasing reports highlighted the existence of extramedullary relapses, which involve skin and
463 soft tissues (Harris *et al.*, 2013).

464 Finally, our findings, linking ZEB1 to AML immune suppression, are mirrored in solid tumors
465 where EMT factors contribute to immune evasion (Terry et al., 2017) (Dongre et al., 2017)
466 (Plaschka et al., 2022), and highlights the need to further investigate the molecular mechanisms
467 by which tumor intrinsic EMT-related pathways affect the microenvironment. The study
468 suggests that EMT/ZEB1 could be a candidate predictive marker to be targeted using specific
469 approaches.

470

471

472

473 **Acknowledgements:** We thank Dr. Maria Teresa Majorini and Dr. Matteo Dugo for
474 bioinformatic assistance and Matteo Milani for preliminary analysis. We thank Dr.
475 Pagani M., Dr. Della Chiara G. and Dr. Bason R. for technical assistance with Chip-
476 qPCR experiments. The authors also thank Ester Grande for providing administrative
477 support. We thank HOVON for sharing data relative to the AML cohort included in the
478 GSE6891.

479

480 **Author contributions:** **B. Bassani:** performed cell culture, molecular experiments,
481 flow cytometry experiments, statistical analysis and contributed to draft the manuscript.
482 **V. Cancila and A. Gulino:** performed IHC experiments. **M. Ciciarello:** revised the
483 manuscript. **C. Chiodoni and D. Lecis:** performed stable Zeb1 silencing and revised
484 the manuscript. **G. Simonetti, A. Piva and E. Fonzi:** performed bioinformatics
485 analysis. **L. Botti:** performed *in-vivo* experiments. **P. Portararo:** performed
486 experiments on MDSCs and suppression assay. **M. Costanza:** performed ELISA assay
487 for Il-2. **J. Schwaller, A. Tzankov, M. Ponzoni, F. Ciceri, N. Bolli and A. Curti**
488 revised the manuscript. **A. Tzankov** also provided the independent cohort of 24
489 patients, performed IHC experiments and analyzed the results. **C. Tripodo:** supervised
490 IHC experiments and revised the manuscript. **M.P. Colombo:** critically discussed data
491 and revised the manuscript. **S. Sangaletti:** conceived the study, analyzed the data,
492 performed statistical analysis and wrote the manuscript.

493 All authors read and approved the final manuscript.

494

495

496

497 **REFERENCES**

498 Almotiri, A., Alzahrani, H., Menendez-Gonzalez, J.B., Abdelfattah, A., Alotaibi, B.,
499 Saleh, L., Greene, A., Georgiou, M., Gibbs, A., Alsayari, A., et al. (2021). Zeb1
500 modulates hematopoietic stem cell fates required for suppressing acute myeloid
501 leukemia. *J Clin Invest* 131. 10.1172/JCI129115.

502 Cancer Genome Atlas Research, N., Ley, T.J., Miller, C., Ding, L., Raphael, B.J.,
503 Mungall, A.J., Robertson, A., Hoadley, K., Triche, T.J., Jr., Laird, P.W., et al. (2013).
504 Genomic and epigenomic landscapes of adult de novo acute myeloid leukemia. *N Engl*
505 *J Med* 368, 2059-2074. 10.1056/NEJMoa1301689.

506 Caramel, J., Ligier, M., and Puisieux, A. (2018). Pleiotropic Roles for ZEB1 in Cancer.
507 *Cancer Res* 78, 30-35. 10.1158/0008-5472.CAN-17-2476.

508 Chen, L., Gibbons, D.L., Goswami, S., Cortez, M.A., Ahn, Y.H., Byers, L.A., Zhang,
509 X., Yi, X., Dwyer, D., Lin, W., et al. (2014). Metastasis is regulated via microRNA-
510 200/ZEB1 axis control of tumour cell PD-L1 expression and intratumoral
511 immunosuppression. *Nat Commun* 5, 5241. 10.1038/ncomms6241.

512 Civini, S., Jin, P., Ren, J., Sabatino, M., Castiello, L., Jin, J., Wang, H., Zhao, Y.,
513 Marincola, F., and Stroncek, D. (2013). Leukemia cells induce changes in human bone
514 marrow stromal cells. *J Transl Med* 11, 298. 10.1186/1479-5876-11-298.

515 Corradi, G., Bassani, B., Simonetti, G., Sangaletti, S., Vadakekolathu, J., Fontana,
516 M.C., Pazzaglia, M., Gulino, A., Tripodo, C., Cristiano, G., et al. (2022). Release of
517 IFN-gamma by acute myeloid leukemia cells remodels bone marrow immune
518 microenvironment by inducing regulatory T cells. *Clin Cancer Res*. 10.1158/1078-
519 0432.CCR-21-3594.

520 Cortes, M., Sanchez-Moral, L., de Barrios, O., Fernandez-Acenero, M.J., Martinez-
521 Campanario, M.C., Esteve-Codina, A., Darling, D.S., Gyorffy, B., Lawrence, T., Dean,
522 D.C., and Postigo, A. (2017). Tumor-associated macrophages (TAMs) depend on
523 ZEB1 for their cancer-promoting roles. *Embo J* 36, 3336-3355.
524 10.15252/embj.201797345.

525 Curti, A., Salvestrini, V., Aluigi, M., Trabanelli, S., Ottaviani, E., Durelli, I.,
526 Horenstein, A.L., Fiore, F., Massaia, M., Piccioli, M., et al. (2007). Modulation of
527 tryptophan catabolism by acute myeloid leukemia cells acts as a general mechanism of
528 immune tolerance via the induction of T regulatory cells. *Blood* 110, 405a-405a. DOI
529 10.1182/blood.V110.11.1345.1345.

530 Davidson-Moncada, J., Viboch, E., Church, S.E., Warren, S.E., and Rutella, S. (2018).
531 Dissecting the Immune Landscape of Acute Myeloid Leukemia. *Biomedicines* 6.
532 10.3390/biomedicines6040110.

533 Dongre, A., Rashidian, M., Reinhardt, F., Bagnato, A., Keckesova, Z., Ploegh, H.L.,
534 and Weinberg, R.A. (2017). Epithelial-to-Mesenchymal Transition Contributes to
535 Immunosuppression in Breast Carcinomas. *Cancer Res* 77, 3982-3989. 10.1158/0008-
536 5472.CAN-16-3292.

537 Dowling, J.K., Afzal, R., Gearing, L.J., Cervantes-Silva, M.P., Annett, S., Davis, G.M.,
538 De Santi, C., Assmann, N., Dettmer, K., Gough, D.J., et al. (2021). Mitochondrial
539 arginase-2 is essential for IL-10 metabolic reprogramming of inflammatory
540 macrophages. *Nat Commun* 12, 1460. 10.1038/s41467-021-21617-2.

541 Feng, S., Cen, J., Huang, Y., Shen, H., Yao, L., Wang, Y., and Chen, Z. (2011). Matrix
542 metalloproteinase-2 and -9 secreted by leukemic cells increase the permeability of
543 blood-brain barrier by disrupting tight junction proteins. *PLoS One* 6, e20599.
544 10.1371/journal.pone.0020599.

545 Geginat, J., Paroni, M., Kastirr, I., Larghi, P., Pagani, M., and Abrignani, S. (2016).
546 Reverse plasticity: TGF-beta and IL-6 induce Th1-to-Th17-cell transdifferentiation in
547 the gut. *Eur J Immunol* *46*, 2306-2310. 10.1002/eji.201646618.

548 Grzywa, T.M., Sosnowska, A., Matryba, P., Rydzynska, Z., Jasinski, M., Nowis, D.,
549 and Golab, J. (2020). Myeloid Cell-Derived Arginase in Cancer Immune Response.
550 *Front Immunol* *11*, 938. 10.3389/fimmu.2020.00938.

551 Hackl, H., Steinleitner, K., Lind, K., Hofer, S., Tosic, N., Pavlovic, S., Suvajdzic, N.,
552 Sill, H., and Wieser, R. (2015). A gene expression profile associated with relapse of
553 cytogenetically normal acute myeloid leukemia is enriched for leukemia stem cell
554 genes. *Leuk Lymphoma* *56*, 1126-1128. 10.3109/10428194.2014.944523.

555 Han, Y., Ye, A., Bi, L., Wu, J., Yu, K., and Zhang, S. (2014). Th17 cells and interleukin-
556 17 increase with poor prognosis in patients with acute myeloid leukemia. *Cancer Sci*
557 *105*, 933-942. 10.1111/cas.12459.

558 Harris, A.C., Kitko, C.L., Couriel, D.R., Braun, T.M., Choi, S.W., Magenau, J.,
559 Mineishi, S., Pawarode, A., Yanik, G., and Levine, J.E. (2013). Extramedullary relapse
560 of acute myeloid leukemia following allogeneic hematopoietic stem cell
561 transplantation: incidence, risk factors and outcomes. *Haematologica* *98*, 179-184.
562 10.3324/haematol.2012.073189.

563 Lamble, A.J., Kosaka, Y., Laderas, T., Maffit, A., Kaempf, A., Brady, L.K., Wang, W.,
564 Long, N., Saultz, J.N., Mori, M., et al. (2020). Reversible suppression of T cell function
565 in the bone marrow microenvironment of acute myeloid leukemia. *Proc Natl Acad Sci
566 U S A* *117*, 14331-14341. 10.1073/pnas.1916206117.

567 Li, L., Feng, Y., Hu, S., Du, Y., Xu, X., Zhang, M., Peng, X., and Chen, F. (2021).
568 ZEB1 serves as an oncogene in acute myeloid leukaemia via regulating the
569 PTEN/PI3K/AKT signalling pathway by combining with P53. *J Cell Mol Med* *25*,
570 5295-5304. 10.1111/jcmm.16539.

571 Li, Z., Herold, T., He, C., Valk, P.J., Chen, P., Jurinovic, V., Mansmann, U.,
572 Radmacher, M.D., Maharry, K.S., Sun, M., et al. (2013). Identification of a 24-gene
573 prognostic signature that improves the European LeukemiaNet risk classification of
574 acute myeloid leukemia: an international collaborative study. *J Clin Oncol* *31*, 1172-
575 1181. 10.1200/JCO.2012.44.3184.

576 Li, Z., Philip, M., and Ferrell, P.B. (2020). Alterations of T-cell-mediated immunity in
577 acute myeloid leukemia. *Oncogene* *39*, 3611-3619. 10.1038/s41388-020-1239-y.

578 Meidhof, S., Brabertz, S., Lehmann, W., Preca, B.T., Mock, K., Ruh, M., Schuler, J.,
579 Berthold, M., Weber, A., Burk, U., et al. (2015). ZEB1-associated drug resistance in
580 cancer cells is reversed by the class I HDAC inhibitor mocetinostat. *EMBO Mol Med*
581 *7*, 831-847. 10.15252/emmm.201404396.

582 Mendez-Ferrer, S., Bonnet, D., Steensma, D.P., Hasserjian, R.P., Ghobrial, I.M.,
583 Gribben, J.G., Andreeff, M., and Krause, D.S. (2020). Bone marrow niches in
584 haematological malignancies. *Nat Rev Cancer* *20*, 285-298. 10.1038/s41568-020-0245-
585 2.

586 Miller, J.A., Cai, C., Langfelder, P., Geschwind, D.H., Kurian, S.M., Salomon, D.R.,
587 and Horvath, S. (2011). Strategies for aggregating gene expression data: the
588 collapseRows R function. *BMC Bioinformatics* *12*, 322. 10.1186/1471-2105-12-322.

589 Mopin, A., Driss, V., and Brinster, C. (2016). A Detailed Protocol for Characterizing
590 the Murine C1498 Cell Line and its Associated Leukemia Mouse Model. *J Vis Exp*
591 10.3791/54270.

592 Mussai, F., De Santo, C., Abu-Dayyeh, I., Booth, S., Quek, L., McEwen-Smith, R.M.,
593 Qureshi, A., Dazzi, F., Vyas, P., and Cerundolo, V. (2013). Acute myeloid leukemia

594 creates an arginase-dependent immunosuppressive microenvironment. *Blood* *122*, 749-
595 758. 10.1182/blood-2013-01-480129.

596 Mussai, F., Wheat, R., Sarrou, E., Booth, S., Stavrou, V., Fultang, L., Perry, T., Kearns,
597 P., Cheng, P., Keeshan, K., et al. (2019). Targeting the arginine metabolic brake
598 enhances immunotherapy for leukaemia. *Int J Cancer* *145*, 2201-2208.
599 10.1002/ijc.32028.

600 Musuraca, G., De Matteis, S., Napolitano, R., Papayannidis, C., Guadagnuolo, V.,
601 Fabbri, F., Cangini, D., Ceccolini, M., Giannini, M.B., Lucchesi, A., et al. (2015). IL-
602 17/IL-10 double-producing T cells: new link between infections, immunosuppression
603 and acute myeloid leukemia. *J Transl Med* *13*, 229. 10.1186/s12967-015-0590-1.

604 Phipson, B., Lee, S., Majewski, I.J., Alexander, W.S., and Smyth, G.K. (2016). Robust
605 Hyperparameter Estimation Protects against Hypervariable Genes and Improves Power
606 to Detect Differential Expression. *Ann Appl Stat* *10*, 946-963. 10.1214/16-AOAS920.

607 Pirillo, C., Birch, F., Tissot, F.S., Anton, S.G., Haltalli, M., Tini, V., Kong, I., Piot, C.,
608 Partridge, B., Pospori, C., et al. (2022). Metalloproteinase inhibition reduces AML
609 growth, prevents stem cell loss, and improves chemotherapy effectiveness. *Blood Adv*
610 *6*, 3126-3141. 10.1182/bloodadvances.2021004321.

611 Plaschka, M., Benboubker, V., Grimont, M., Berthet, J., Tonon, L., Lopez, J., Le-
612 Bouar, M., Balme, B., Tondeur, G., de la Fouchardiere, A., et al. (2022). ZEB1
613 transcription factor promotes immune escape in melanoma. *J Immunother Cancer* *10*.
614 10.1136/jitc-2021-003484.

615 Sangaletti, S., Tripodo, C., Chiodoni, C., Guarnotta, C., Cappetti, B., Casalini, P.,
616 Piconese, S., Parenza, M., Guiducci, C., Vitali, C., and Colombo, M.P. (2012).
617 Neutrophil extracellular traps mediate transfer of cytoplasmic neutrophil antigens to
618 myeloid dendritic cells toward ANCA induction and associated autoimmunity. *Blood*
619 *120*, 3007-3018. 10.1182/blood-2012-03-416156.

620 Sangaletti, S., Tripodo, C., Santangelo, A., Castioni, N., Portararo, P., Gulino, A., Botti,
621 L., Parenza, M., Cappetti, B., Orlandi, R., et al. (2016). Mesenchymal Transition of
622 High-Grade Breast Carcinomas Depends on Extracellular Matrix Control of Myeloid
623 Suppressor Cell Activity. *Cell Rep* *17*, 233-248. 10.1016/j.celrep.2016.08.075.

624 Scott, C.L., and Omilusik, K.D. (2019). ZEBs: Novel Players in Immune Cell
625 Development and Function. *Trends Immunol* *40*, 431-446. 10.1016/j.it.2019.03.001.

626 Shousha, W.G., Ramadan, S.S., El-Saiid, A.S., Abdelmoneim, A.E., and Abbas, M.A.
627 (2019). Expression and clinical significance of SNAI1 and ZEB1 genes in acute
628 myeloid leukemia patients. *Mol Biol Rep* *46*, 4625-4630. 10.1007/s11033-019-04839-
629 y.

630 Simonetti, G., Angeli, D., Petracci, E., Fonzi, E., Vedovato, S., Sperotto, A., Padella,
631 A., Ghetti, M., Ferrari, A., Robustelli, V., et al. (2021). Adrenomedullin Expression
632 Characterizes Leukemia Stem Cells and Associates With an Inflammatory Signature in
633 Acute Myeloid Leukemia. *Front Oncol* *11*, 684396. 10.3389/fonc.2021.684396.

634 Stavropoulou, V., Kaspar, S., Brault, L., Sanders, M.A., Juge, S., Morettini, S.,
635 Tzankov, A., Iacovino, M., Lau, I.J., Milne, T.A., et al. (2016). MLL-AF9 Expression
636 in Hematopoietic Stem Cells Drives a Highly Invasive AML Expressing EMT-Related
637 Genes Linked to Poor Outcome. *Cancer Cell* *30*, 43-58. 10.1016/j.ccr.2016.05.011.

638 Stritesky, G.L., Yeh, N., and Kaplan, M.H. (2008). IL-23 promotes maintenance but
639 not commitment to the Th17 lineage. *J Immunol* *181*, 5948-5955.
640 10.4049/jimmunol.181.9.5948.

641 Subramanian, A., Tamayo, P., Mootha, V.K., Mukherjee, S., Ebert, B.L., Gillette,
642 M.A., Paulovich, A., Pomeroy, S.L., Golub, T.R., Lander, E.S., and Mesirov, J.P.
643 (2005). Gene set enrichment analysis: a knowledge-based approach for interpreting

644 genome-wide expression profiles. *Proc Natl Acad Sci U S A* *102*, 15545-15550.
645 10.1073/pnas.0506580102.

646 Terry, S., Savagner, P., Ortiz-Cuaran, S., Mahjoubi, L., Saintigny, P., Thiery, J.P., and
647 Chouaib, S. (2017). New insights into the role of EMT in tumor immune escape. *Mol
648 Oncol* *11*, 824-846. 10.1002/1878-0261.12093.

649 Tettamanti, S., Pievani, A., Biondi, A., Dotti, G., and Serafini, M. (2021). Catch me if
650 you can: how AML and its niche escape immunotherapy. *Leukemia*. 10.1038/s41375-
651 021-01350-x.

652 Thol, F., and Ganser, A. (2020). Treatment of Relapsed Acute Myeloid Leukemia. *Curr
653 Treat Options Oncol* *21*, 66. 10.1007/s11864-020-00765-5.

654 Tomida, M. (1995). Induction of differentiation of WEHI-3B D+ leukemic cells
655 transfected with differentiation-stimulating factor/leukemia inhibitory factor receptor
656 cDNA. *Blood* *85*, 217-221.

657 Tyner, J.W., Tognon, C.E., Bottomly, D., Wilmot, B., Kurtz, S.E., Savage, S.L., Long,
658 Schultz, A.R., Traer, E., Abel, M., et al. (2018). Functional genomic landscape of
659 acute myeloid leukaemia. *Nature* *562*, 526-531. 10.1038/s41586-018-0623-z.

660 Vadakekolathu, J., Minden, M.D., Hood, T., Church, S.E., Reeder, S., Altmann, H.,
661 Sullivan, A.H., Viboch, E.J., Patel, T., Ibrahimova, N., et al. (2020). Immune
662 landscapes predict chemotherapy resistance and immunotherapy response in acute
663 myeloid leukemia. *Sci Transl Med* *12*. 10.1126/scitranslmed.aaz0463.

664 van Vlerken-Ysla, L., Tyurina, Y.Y., Kagan, V.E., and Gabrilovich, D.I. (2023).
665 Functional states of myeloid cells in cancer. *Cancer Cell*. 10.1016/j.ccr.2023.02.009.

666 Verhaak, R.G., Wouters, B.J., Erpelinck, C.A., Abbas, S., Beverloo, H.B., Lugthart, S.,
667 Lowenberg, B., Delwel, R., and Valk, P.J. (2009). Prediction of molecular subtypes in
668 acute myeloid leukemia based on gene expression profiling. *Haematologica* *94*, 131-
669 134. 10.3324/haematol.13299.

670 Vitali, C., Bassani, C., Chiodoni, C., Fellini, E., Guarnotta, C., Miotti, S., Sangaletti,
671 S., Fuligni, F., De Cecco, L., Piccaluga, P.P., et al. (2015a). SOCS2 Controls
672 Proliferation and Stemness of Hematopoietic Cells under Stress Conditions and Its
673 Deregulation Marks Unfavorable Acute Leukemias. *Cancer Res* *75*, 2387-2399.
674 10.1158/0008-5472.CAN-14-3625.

675 Vitali, C., Tripodo, C., and Colombo, M.P. (2015b). MEF2C and SOCS2 in stemness
676 regulation. *Oncoscience* *2*, 936-937. 10.18632/oncoscience.279.

677 Wu, H., Zhen, Y., Ma, Z., Li, H., Yu, J., Xu, Z.G., Wang, X.Y., Yi, H., and Yang, Y.G.
678 (2016). Arginase-1-dependent promotion of TH17 differentiation and disease
679 progression by MDSCs in systemic lupus erythematosus. *Sci Transl Med* *8*, 331ra340.
680 10.1126/scitranslmed.aae0482.

681

682

683

684 **FIGURE LEGENDS**

685

686 **Figure 1. The median of *ZEB1* expression dichotomizes AML patients and defines**
687 **patients with peculiar immune features and worse OS. A.** *ZEB1* expression levels in
688 the GEP analysis performed combining 7 independent AML cohorts (GSE15434, GSE16015,
689 GSE12417, GSE37642, GSE6891, GSE161532 and TCGA) for a total of 1325 AML patients.
690 **B.** Relevant pathways associated with *ZEB1*^{high} and *ZEB1*^{low} AML blasts in the 7 cohorts. **C.**
691 Expression of selected differentially expressed genes (*MYC*, *SOCS2* and *ARG2*) in *ZEB1*^{high} and
692 *ZEB1*^{low} AML patients. **D.** Kaplan-Mayer curves showing *ZEB1*^{high} and *ZEB1*^{low} patients overall
693 survival (OS) combining the AML cohorts for which OS data were available (GSE12417,
694 GSE37642, GSE6891, GSE161532 and TCGA for a total of 1298 patients.
695

696

697 **Figure 2. Zeb1 silencing impairs the invasive ability of leukemic C1498 cells without**
698 **affecting their proliferation. A.** Western blot analysis showing *ZEB1* expression in WEHI-
699 3B and C1498 murine AML cell lines. BM-derived mesenchymal stem cells (MSC) isolated
700 from BALB/c (B/c) mice were used as *ZEB1* positive control. β -actin was used as internal
701 control. **B.** qPCR showing basal levels of *Zeb1* in WEHI-3B and C1498 murine AML cell lines.
702 β -actin was used as internal control. (n=4, one experiment out of 2 performed, p=0.0050;
703 Unpaired t test **p<0.01). **C.** qPCR showing the expression of *Arg1* and *Tgfb* in C1498 and
704 WEHI-3B cell lines. Results represent a pool of at least 2 independent experiments **D.** Stable
705 knockdown of *Zeb1* in C1498 using lentiviral vectors evaluated by Western Blot. β -actin was
706 used as internal control **E.** XTT proliferation assay performed on *Zeb1* expressing (Scr) and
707 silenced cell lines. Cell proliferation for each time point was calculated as the (Absorbance
708 (Abs) at 450nm – Abs at 670nm) t 24/48/72)/ (Abs at 450nm –Abs at 670nm) t 0 *100. Data
709 represent a pool of 2 independent experiments; n=12/each experiment). **F.** *In-vitro* invasion
710 assay using 24-well transwell plates (5 μ m pore size) coated with 1 mg/ml Matrigel growth
711 factor reduced basement membrane matrix. Five consecutive fields per transwell were counted.
712 (n=3/each; one-way ANOVA; KW test p=0.0064). **G.** *Tgfb* and **H.** *Arg1* expression levels in
713 *ZEB1* expressing (Scramble) and silenced cell lines. β -actin was used as internal control. **I.**
714 Volcano plot showing the up-regulated and down-regulated genes in Scramble vs and silenced
715 cells. **J.** Heatmap of canonical pathway enrichment analysis performed on *Zeb1* expressing vs
716 silenced (sh*Zeb1*-seq C and sh*Zeb1*-seq D respectively) cells **K.** Suppression assay performed
717 with Scramble and sh*Zeb1*-seq D silenced cells where irradiated C1498 cells were co-cultured
718 with α CD3- α CD28 stimulated CFSE-labelled T-cells (total splenocytes) at different ratio.
719 CD4 $^{+}$ and CD8 $^{+}$ proliferation was assessed 48h after. Data represent 1 experiment out of 3
performed (n=3/dilution; statistical analysis: unpaired t test ****p<0.0001). **L.** *ZEB1* IHC

720 staining performed on the spleens explanted from naïve or tumor bearing (breast cancer) mice.
721 Original magnification, x200 and x630 (insets). Scale bar, 50 μ m. **M.** ZEB1 IHC staining in
722 MDSC isolated from mice bearing mammary tumors and N1 neutrophils isolated from agar
723 plugs. **N.** *Zeb1* transient silencing (48h) in MDSCs sorted from tumor bearing mice. *Arg1* and
724 *Il2* expression levels in *Zeb1* silenced and Scramble control MDSCs. Untreated MDSCs were
725 used as further negative control. Statistical analysis: One way ANOVA followed by Tukey's
726 multiple comparison. The p value relative to the comparison Scramble vs siRNA is shown in
727 the figure (p=0.024 for *Arg1* and p=0.019 for *Il2*) **O.** *Il2* levels detected by ELISA assay in
728 *Zeb1* silenced MDSC and Scramble control supernatants. (*p< 0.05; **p< 0.01; ***p<0.001;
729 ****p<0.0001)

730

731 **Figure 3. Zeb1 down-regulation was associated with the promotion of a cytotoxic**
732 **microenvironment.** **A.** Scramble (n=32) and sh*Zeb1*-seq D (n=26) were injected in the tibia of
733 immunocompetent C57BL/6 mice and the percentage of GFP+ cells within the BM was
734 evaluated with flow cytometry 34days post injection. Naïve mice (n=5) were used as controls.
735 Data represent a pool of 3 independent experiments (Statistic: One-way ANOVA; for multiple
736 comparison ****p<0.0001; KW test p<0.0001). **B.** Representative hematoxylin and eosin
737 staining of liver explanted from Scramble -injected and sh*Zeb1*-seq D injected mice. 10X and
738 20X magnifications are shown. **C.** Extramedullary disease area quantification of liver explanted
739 by Scramble -injected and sh*Zeb1*-seq D injected mice. Data represent the quantification of an
740 individual experiment (n=5; unpaired t test; p=0.09). **D.** Frequencies of CD8⁺PD1⁺ within the
741 BM of control mice (CTRLB6, n=9) or mice injected with *Zeb1*-expressing (Scramble, n=37)
742 or silenced cells (sh*Zeb1*-seqD, n=31). Data represent a pool of 3 independent experiments
743 (Statistical Analysis: One-way ANOVA followed by Tukey's multiple comparison, p=0.0001;
744 the p values relative to the comparisons Scramble vs CTRL or vs sh*Zeb1* seq D are shown in
745 the figure; *p<0.05). **E.** Frequencies of CD8⁺IFN- γ ⁺ within the BM of control mice (CTRL B6,
746 n=9) or mice injected with *Zeb1*-expressing (Scramble, n=39) or silenced cells (sh*Zeb1*-seqD,
747 n=35). Data represent a pool of 3 independent experiments, (Statistical Analysis: one-way
748 ANOVA followed by Tukey's multiple comparison, p=0.0004; the p value relative to the
749 comparisons Scramble vs sh*Zeb1* seq D are shown in the figure; ***p<0.001). **F.** Frequencies
750 of total CD8⁺PD1⁺Ki67⁺IFN- γ ⁺ cells within the BM of control mice (CTRL B6, n=9) or mice
751 injected with *Zeb1*-expressing (Scramble, n=39) or silenced cells (sh*Zeb1*-seqD, n=23). Data
752 represent a pool of 2 independent experiments. (statistical Analysis: one-way ANOVA
753 followed by Tukey's multiple comparison, p=0.0038; the p value relative to the comparisons
754 Scramble vs sh*Zeb1* seq D is shown in the figure; *p<0.05). **G.** Frequencies of CD8 exhausted
755 (PD1⁺TIM3⁺) cells within the BM of control mice (CTRLB6, n=5) or mice injected with *Zeb1*-

756 expressing (Scramble, n=6) or silenced cells (shZeb1-seqD, n=12). statistical Analysis: one-
757 way ANOVA followed by Tukey's multiple comparison, p=0.0178; the p value relative to the
758 comparisons Scramble vs CTRL or Zeb D is shown in the figure; *p<0.05 **H**. Percentage of
759 CD8⁺OX40⁺lymphocytes within the BM of mice (CTRL B6, n=9, Scramble, n=22, shZeb1-seq
760 D, n=26). Data represent a pool of 2 independent experiments (statistical Analysis: one-way
761 ANOVA followed by Tukey's multiple comparison, p=0.0009; the p value relative to the
762 comparisons Scramble vs shZeb1 seq D is shown in the figure; **p<0.01). mRNA levels of **I**.
763 *Perforin1 (Prf1)* (KW test, p=0.001; *p<0.05); **J**. *Granzyme B (Gzmb)*; **K**. *Ox40l (Thsf4)* (KW
764 test, p=0.002; **p<0.001) and **L**. *Tnf*. **M**. *Arginase 1 (Arg1)* (KW test, p=0.0133; *p<0.05) and
765 **N**. *Il10* (KW test, p=0.0458; *p<0.05) within the BM of mice injected with C1498 expressing
766 (n= 8) or silenced for Zeb1 (n=11). BM of naïve mice (n=3) was used as control.
767

768 **Figure 4. – Zeb1 expression is associated with an expansion of lymphocytes producing IL-
769 17A that in turn promotes AML aggressiveness.** **A**. Frequency of Treg (CD4⁺CD25⁺Foxp3⁺)
770 within the BM of control mice (CTRL B6, n=9) or mice injected with ZEB1-expressing
771 (Scramble, n=31) or silenced cells (shZeb1-seqD, n=28). Data represent a pool of 2 independent
772 experiments. Frequency of activated CD4 lymphocytes producing **B**. TNF and **C**. IFN- γ (CTRL
773 B6, n=9, Scramble, n=21, shZeb1-seq D, n=25). Data represent a pool of 2 independent
774 experiments Statistic: KW test, p=0.0388; For the multiple comparisons: *p<0.05; **D**.
775 Frequency of IL-17⁺ CD3⁺ cells (CTRL B6, n=3, Scramble, n=16, shZeb1-seq D, n=17),
776 Statistic: KW test, p=0.0289; For the multiple comparisons: *p<0.05. **E**. IL-17⁺ CD4⁺ cells
777 (CTRL B6, n=5, Scramble, n=21, shZeb1-seq D, n=17; Statistic: KW test, p=0.0115; For the
778 multiple comparisons: *p<0.05) and of **F**. Treg (CD4⁺CD25⁺Foxp3⁺) producing IL-17A
779 (CTRL B6, n=5, Scramble, n=25, shZeb1-seq D, n=19). Statistic: KW test, p=0.0005; For the
780 multiple comparisons: *p<0.05; ***p<0.001. **G**. *Il6* (statistic: ANOVA, Tukey's multiple
781 comparison test; ***p<0.001;****p<0.0001), and *Il23* (statistic: ANOVA, Tukey's multiple
782 comparison test; *p<0.05; **p<0.01) expression levels in silenced cells and Scramble. **H**.
783 Immunocompetent mice were injected with either C1498 Scramble or Zeb1 silenced cells
784 (5x10⁵ cells i.v.) at day 0 and then treated with anti-IL17 neutralizing antibody or its isotype
785 control (50 μ g. i.p.) every 3 days. Mice were sacrificed after 30 days and BM and livers were
786 harvested for FACS analysis. Frequency of GFP+ cells within the **I**. BM and **J**. liver of mice
787 injected with Zeb1 expressing or silenced cells and treated with Isotype control (Scramble
788 n=12, shZeb1 seq C n=4-5, shZeb1 seq D n=7) or α IL-17A (Scramble n=12, shZeb1 seq C
789 n=4-5, shZeb1 seq D n=7) Statistic: Mann-Whitney t test **p<0.01; p=0.0011.

790 **Figure 5. – IL-17A stimulation promotes the expression of genes associated to leukemic
791 cell aggressiveness.** **A.** Cell proliferation of C1498 expressing (scramble) or silenced (shZeb1-
792 seq D) upon IL-17A stimulation (50 ng/mL) assessed by Xtt assay after 24h, 48h and 72h. Cell
793 proliferation for each time point was calculated as the (Absorbance (Abs) at 450 nm – Abs at
794 670 nm). Data represent a pool of 2 experiments (Two-way ANOVA, Multiple comparison
795 test: ** p< 0.01;****p<0.0001). **B.** qPCR showing the induction of *Socs2*, *Mmp9* and **C.** *Tgfb*
796 and *Il6* upon stimulation (7 days) with IL-17A 50 ng/mL in Zeb1 expressing cells. Statistic:
797 Paired *t* test; p=0.0255) **D.** ZEB1 expression in a panel of 6 different leukemic cell lines
798 evaluated by Western Blot. **E.** Stable knockdown of ZEB1 in K562 using lentiviral vectors
799 evaluated by Western Blot. β -actin was used as internal control. **F.** *ZEB1* (p=0.0002), *SOCS2*
800 (p<0.0001), *IL23A* (p=0.0125), and *TGF β* (p=0.0025) expression levels in silenced cells and
801 Scramble. Data represent a pool of 3 experiments (Statistics: Unpaired t test) **G.** qPCR showing
802 the induction of *SOCS2* (*p< 0.05), *MMP9* and **H.** *TGF- β* , *IL6* (**p< 0.01) upon stimulation
803 (7 days) with IL-17A 50 ng/mL in ZEB1 expressing cells.; **I.** Chromatin immunoprecipitation
804 assay of ZEB1 showing the direct binding to SOCS2 and IL23A in K562 cells. The fraction of
805 chromatin bound to the promoter, with IgG negative control or anti-ZEB1 antibody is
806 represented as a percentage of input. Data represent a pool of 2 independent experiments.
807

808 **Figure 6. - ZEB1^{high} levels in AML patients positively correlates with the expansion of
809 IL17+ CD3 cells.** **A.** ZEB1 quantitative analysis of immunohistochemical staining performed
810 using the Image Analysis software provided by Leica ("nuclear hub" tool). (Statistic: Mann-
811 Whitney *t* test****p< 0.0001) **B.** Quantification of CD3+IL-17+ cells within the BM of
812 ZEB1^{high} (n=9) and ZEB1^{low} (n=16) AML patients. (Statistic: Mann-Whitney *t* test****p<
813 0.0001) **C.** Representative immunohistochemical staining for ZEB1 and immunofluorescence
814 for CD3+IL-17A+ evaluation (CD3 in green and IL-17A in red) performed on 26 archival BM
815 biopsy of AML patients (University of Palermo cohort). Original magnification, x200 and
816 x400. Scale bars, 50 and 100 μ m. **D.** Positive correlation between ZEB1 positive cells and
817 CD3+IL-17A+ infiltrate. Statistics: Pearson' correlation; R= 0.6265; p< 0.0001. **E.** Overall
818 survival of AML patients (TCGA) with high and low Th17 infiltration. 16 genes (*CXCL3*, *IL22*,
819 *IL3*, *CCL4*, *GZMB*, *LRMP*, *CCL5*, *CASPI*, *CSF2*, *CCL3*, *TBX21*, *ICOS*, *IL7R*, *STAT4*, *LGALS3*
820 and *LAG3*) were used to define specific cell populations.
821

822 **Figure 7. Relevance of Th17-ZEB1 axis in AML relapse** **A.** *ZEB1* expression levels at
823 diagnosis and relapse in 11 AML patients (GSE66525). Expression levels of **B.** *MMP2* and **C.**
824 *SOCS2* at diagnosis and relapse in GSE66525 **D.** IL-17 enrichment pathway at relapse vs at

825 diagnosis. **E.** hallmark pathways enriched or downregulated in relapsed patients compared with
826 patients at diagnosis.

827

828

829

830

Figure 1

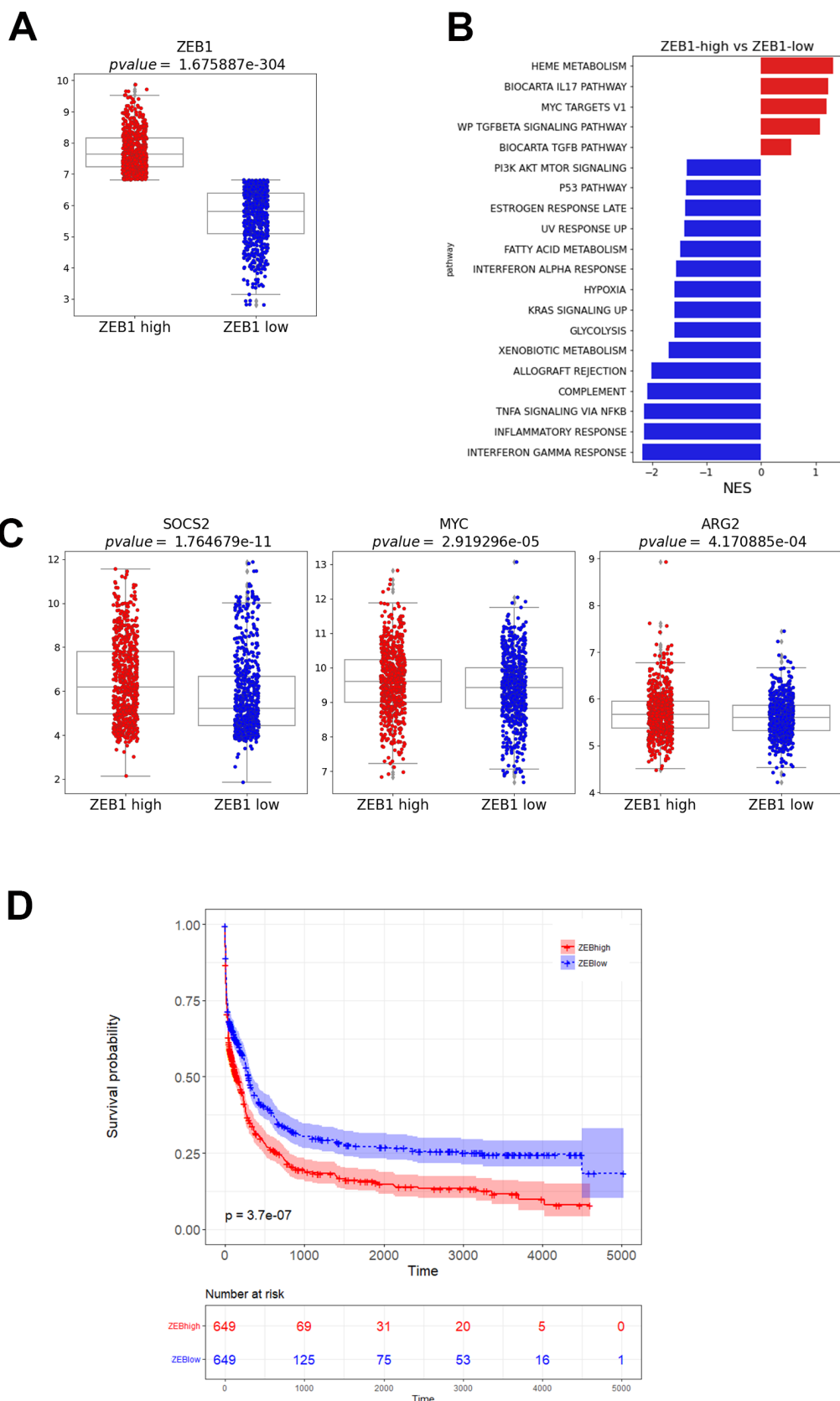


Figure 2

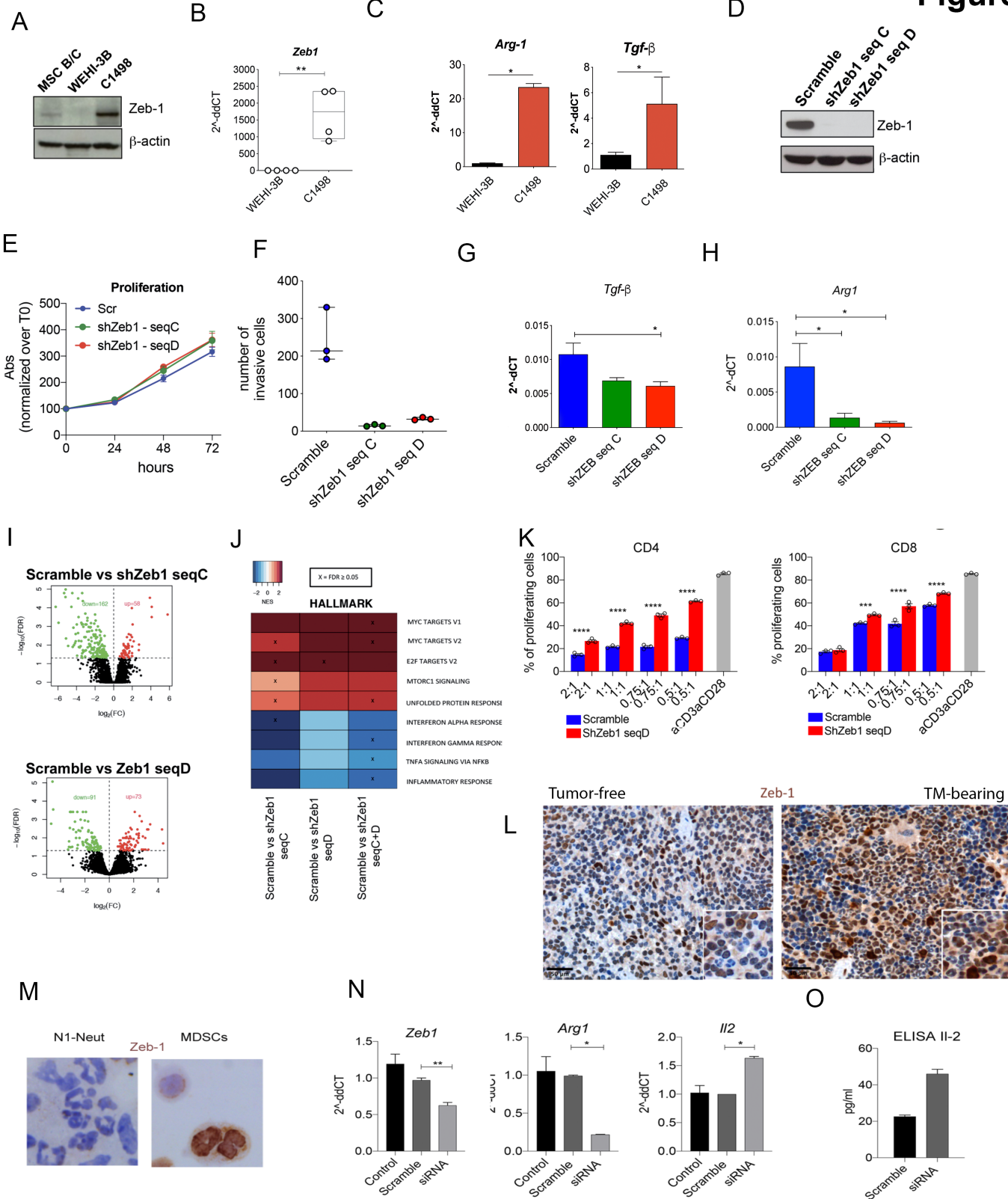


Figure 3

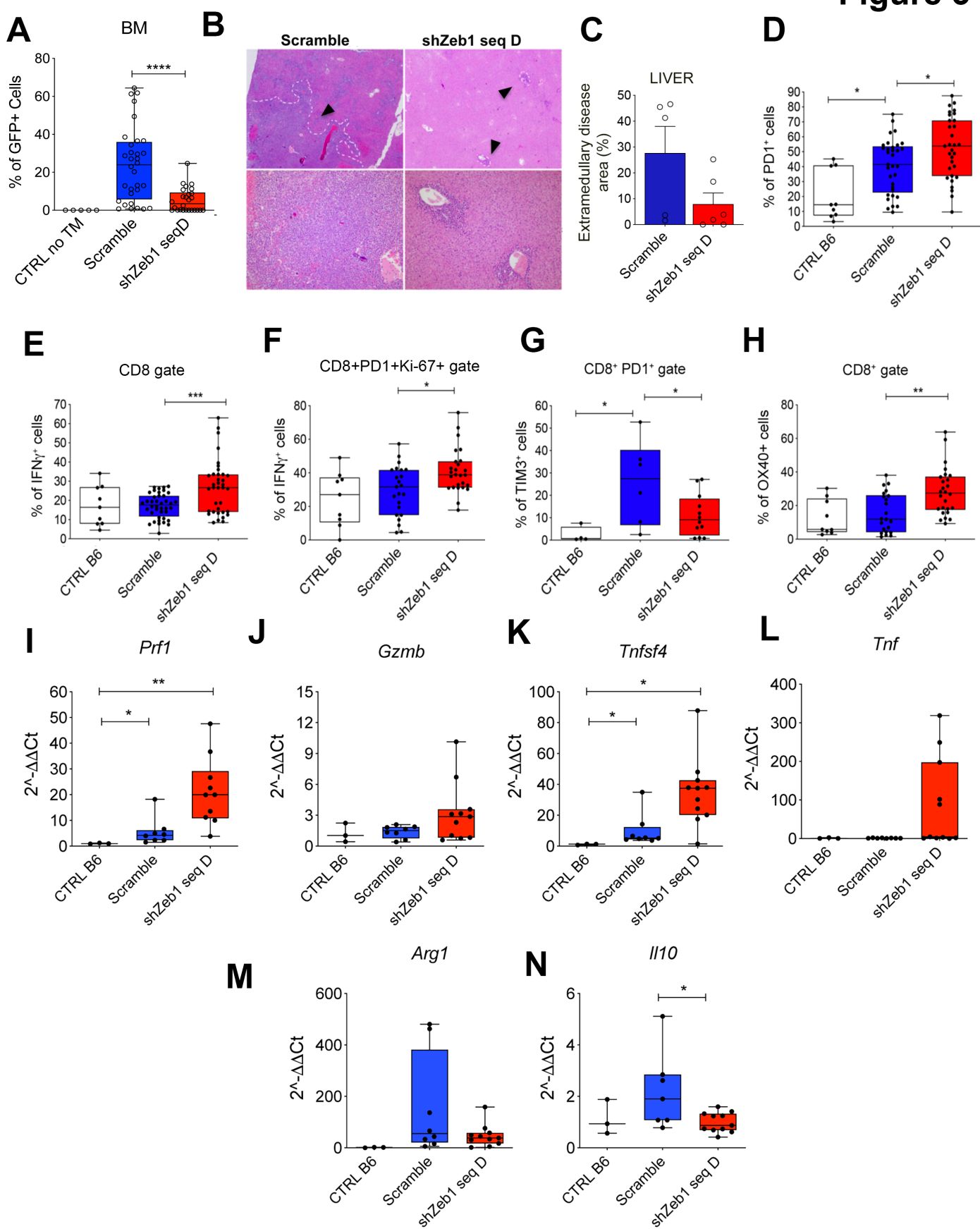


Figure 4

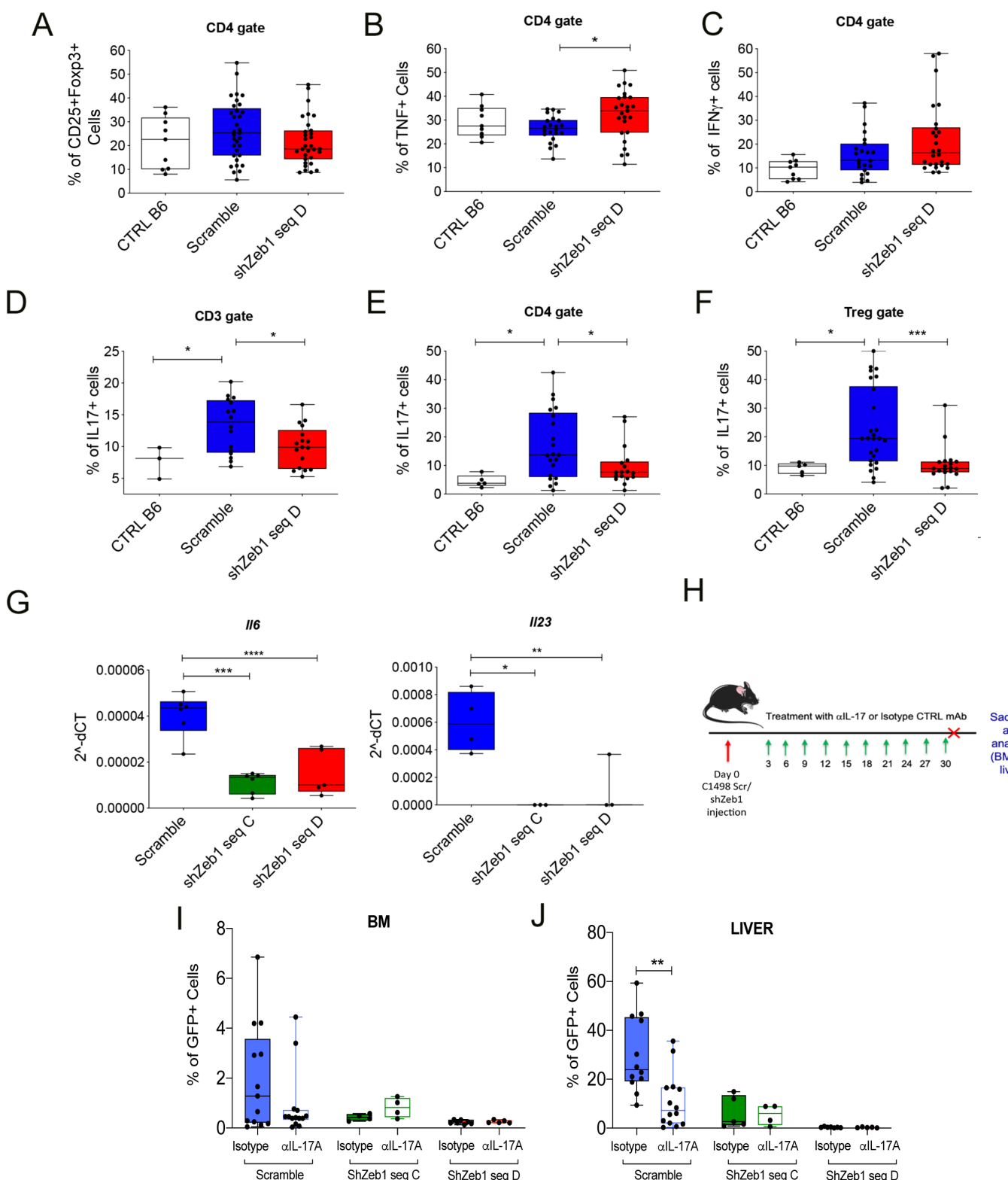


Figure 5

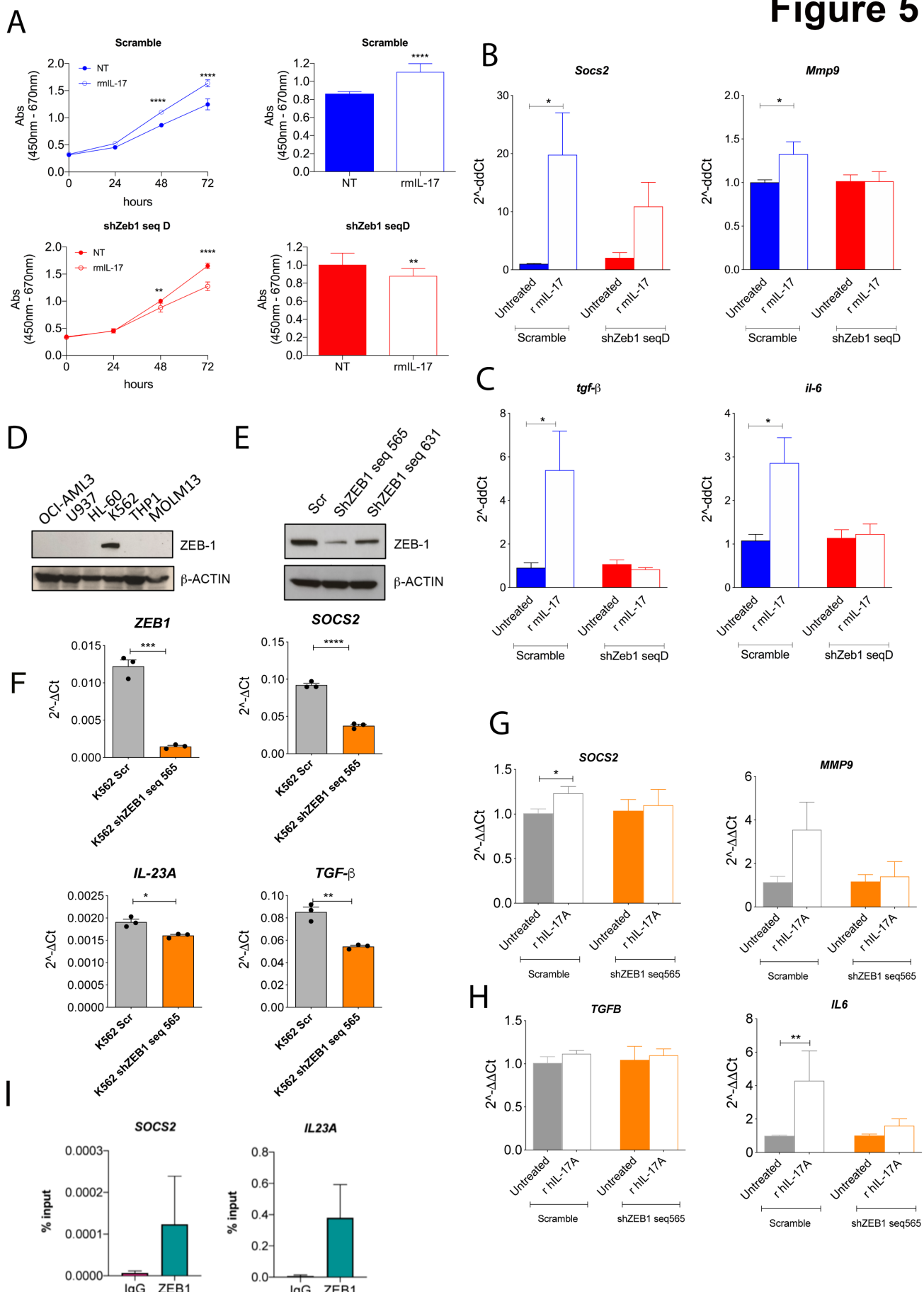


Figure 6

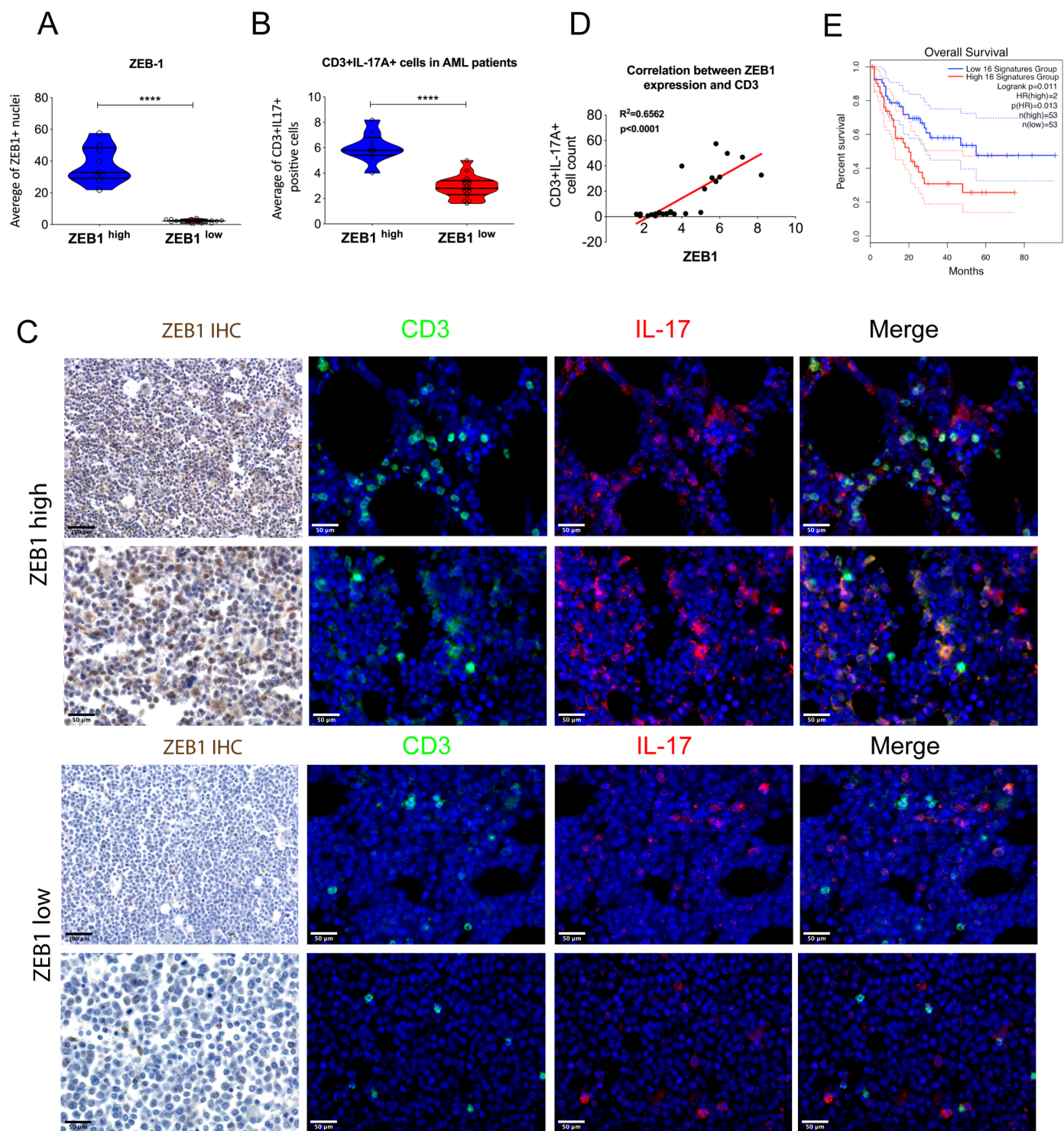


Figure 7

